Development of a correlation ECE radiometer for electron temperature fluctuation measurements in Heliotron J

Gavin M. Weir[1], *Kazunobu* Nagasaki[2,*], *Jinxiang* Zhu[3], *Maoyuan* Luo[4], *Hiroyuki* Okada[2], *Takashi* Minami[2], *Shinichiro* Kado[2], *Shinji* Kobayashi[2], *Satoshi* Yamamoto[2], *Shinsuke* Ohshima[2], *Shigeru* Konoshima[2], *Yuji* Nakamura[4], *Akihiro* Ishizawa[4], *Xiang-xun* Lu[4], *Linge* Zang[5], *Nikolai* Marushchenko[1] and *Yasuo* Yoshimura[6], and *Tohru* Mizuuchi[2]

[1]Max-Planck Institute for Plasma Physics, Greifswald, Germany
[2]Institute of Advanced Energy, Kyoto University, Gokasho, Uji, Kyoto, Japan
[3]Zhejiang University, Hangzhou, China
[4]Graduate School of Energy Science, Kyoto University, Uji, Kyoto, Japan
[5]Southwestern Institute of Physics, Chengdu, China
[6]National Institute for Fusion Science, Toki, Japan

Abstract. A radial correlation ECE radiometer diagnostic has been developed for electron temperature fluctuation measurements in the helical-axis heliotron device, Heliotron J. The radiometer consists of two heterodyne detection systems. One system scans the frequency of a local oscillator from 52 to 64 GHz with a single intermediate frequency filter, and the second system has a fixed frequency, 56 GHz local oscillator with four intermediate frequency filters. This frequency range covers measurement positions spanning from the plasma core to the half radius. Laboratory tests indicate that each system has narrow intermediate frequency bandwidth and high-sensitivity over a large dynamic range. During plasma experiments with NBI heating, radiation temperature fluctuation measured by the CECE radiometer decrease with increasing ECCD commensurate with previous measurements of energetic particle driven modes on Heliotron J.

1 Introduction

Turbulence in density and temperature is believed to govern energy and particle confinement in magnetically confined fusion plasmas. Several theories suggest that turbulent electrostatic and/or electromagnetic fluctuations are responsible for this anomalous transport. Drift wave turbulence has been experimentally and theoretically studied, and Trapped Electron Modes (TEMs) have been found to lead to experimentally relevant electron heat transport [1-3] in tokamak and helical devices.

While plasma density fluctuations may be directly measured in the confinement region with microwave or optical diagnostics, electron temperature fluctuations are measured indirectly through decorrelation of Electron Cyclotron Emission (ECE) [4]. This is necessary because thermal noise dominates electron temperature fluctuations in the ECE spectrum and standard ECE radiometry techniques are not suitable for measuring high-frequency, small amplitude temperature fluctuations.

Progress has been made in extracting electron temperature fluctuations from the dominant thermal noise in tokamaks and helical devices. The first proof-of-principle measurements of core electron temperature fluctuations were reported from the W7-AS stellarator [5] and the TEXT-U tokamak [6-9], and electron temperature fluctuations might contribute significantly to the anomalous electron heat flux when they are correlated with potential fluctuations [10]. Electron temperature and plasma density fluctuations have been measured on the DIII-D and ASDEX Upgrade tokamaks, and the cross phase between the two has been found to be a sensitive indicator of drift wave driven turbulence when compared to nonlinear gyrokinetic simulations of ITG/TEM driven turbulence [11-14]. Correlation ECE radiometry is reviewed in Ref. 4, and four decorrelation schemes are suggested:

1. spatial decorrelation through multiple sightlines of the same plasma volume
2. spectral decorrelation of separate frequency bands along a single sightline
3. spatial decorrelation of disjoint measurement volumes
4. autocorrelation of radiation decorrelated in time

Method (2) is the most commonly used decorrelation scheme; however, method (1) was used on W7-AS stellarator, and (4) was used on the TEXT-U tokamak. A poloidal correlation ECE radiometer using method (3) has been developed for the W7-X stellarator [15].

Recently we have designed and installed a new correlation ECE radiometer system to measure core electron temperature fluctuations on the medium-sized stellarator/heliotron (S/H) device, Heliotron J. The CECE system consists of two separate heterodyne detection systems, and either spectral decorrelation along the same sightline or spatial decorrelation through two toroidally

* Corresponding author: nagasaki@iae.kyoto-u.ac.jp

separated measurement volumes may be used to decorrelate thermal noise in the ECE spectrum.

In this paper, we will concentrate on the spectral decorrelation method and report on the development of a correlation ECE (CECE) radiometer for temperature fluctuations and recent plasma experimental results in the helical-heliotron device, Heliotron J. The organization is as follows: The Heliotron J device and CECE radiometer are described in Sec. 2. Laboratory tests are presented in Sec. 3, and CECE measurements during plasma experiments with ECRH and NBI heating are presented in Sec. 4. A summary of the new CECE diagnostic and its first results is presented in Sec. 5

2 Heliotron J and the CECE diagnostic

2.1. The Heliotron J device

Heliotron J is a medium-sized plasma experimental helical device [16][17]. The average major radius is R=1.2 m, and the average minor radius is a=0.1–0.2 m depending on magnetic configuration. The rotational transform also changes with magnetic configuration, $\iota/2\pi$=0.3–0.8, and the maximum magnetic field strength on the magnetic axis is B=1.5 T. The magnetic coil system is composed of an L = 1/M = 4 helical coil, two types of toroidal coils, and three pairs of vertical coils. Here L and M denote the poloidal and toroidal pitch numbers, respectively. The magnetic configuration of Heliotron J can be changed significantly by varying the current ratios in each coil, allowing us to investigate the properties of global confinement, neoclassical transport, turbulent transport and MHD stability in a wide range of magnetic configurations.

Plasmas are produced and heated by second harmonic X-mode ECH at 70-GHz [18]. The maximum injected EC power is 380 kW, and the focused EC beam radius at $1/e^2$ power is 3 cm at the magnetic axis. This is much smaller than the plasma minor radius, a~17 cm, localizing the power deposition and driven current profiles. A steerable mirror allows the injection angle of the ECRH to varied in the toroidal and poloidal directions, and $N_{||}$ sampled by the ECRH beam ranges from -0.05 to 0.6 for positive magnetic field, limited by the chamber port size. Here $N_{||}$ is the parallel refractive index, determined by the angle between axial magnetic field and EC wave vector under vacuum condition, and positive magnetic field corresponds to the counter-clockwise direction. The EC launcher is positioned between the "straight" and "corner" sections of the non-axisymmetric vacuum vessel. For the extraordinary wave polarization (X-mode) the absorbed power is greater than 80%, and can be larger than 90 % under adequate conditions ($0.1 < N_{||} < 0.6$). In this paper we report results from plasmas with ECRH and NBI heating, where the core electron temperature is measured to be approximately 1 keV and the plasma line-average density is $n_e=1.2\times10^{19}$ m^{-3}.

Figure 1 shows the poloidal cross-section of the Heliotron J plasma at the CECE measurement position. The trajectory of 70 GHz electron cyclotron waves is calculated using the TRAVIS code. The magnetic field of the Heliotron J device has a tokamak-like mod-B contour at the viewing port for the CECE radiometer, and second harmonic X-mode ECE between 52 and 72 GHz radiates from the plasma core to the edge region. The core optical depth is approximately 3 for a plasma with $n_e=1.2\times10^{19}$ m^{-3} and T_e=1.0 keV in Heliotron J, and the average emission from the core is optically thick. The antenna is located at the #11.5 low field side port of the Heliotron J vacuum chamber and is comprised of a pyramidal horn and focusing polytetrafluoroethylene lens with a beamwaist of approximately 2 cm. The detected ECE signal is transmitted to the radiometer with approximately 10 m of oversized rectangular waveguides (X-band). A 70 GHz notch filter (band stop) filter is used to protect the CECE diagnostic by suppressing stray ECRH power.

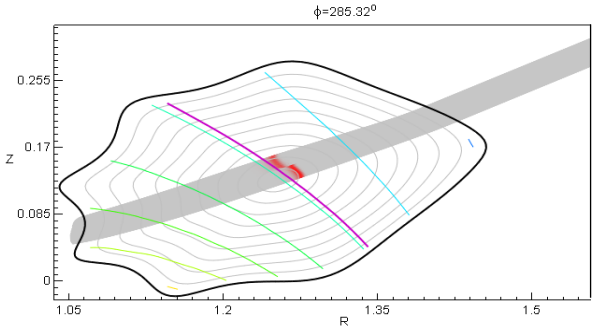

Fig. 1. Poloidal cross-section of Heliotron J at the CECE viewing location. The trajectory of 70 GHz EC waves is calculated using the TRAVIS code.

2.2 Correlation ECE radiometer

A single-sightline correlation electron cyclotron emission (CECE) radiometer has been developed and implemented on Heliotron J for studying bulk electron temperature fluctuations. A conventional multi-channel ECE radiometer is routinely used for electron temperature profile measurements [19], and the new radiometer shares some previously existing components from that system. The new radiometer consists of two detection systems. Figure 2 illustrates a schematic of the CECE radiometer. One detection system (CECE-RF) includes a variable frequency local oscillator (LO) that can be scanned from 52 to 64 GHz with high frequency resolution using a signal generator and a 4-times multiplier. Post-mixing, the down-converted intermediate frequency (IF) signal is bandpass filtered by an 8 GHz intermediate frequency filter with a bandwidth of B_{IF}=0.2 GHz. The filtered IF signal is detected with a crystal diode RF detector, and then amplified with an AC/DC coupling video amplifier. The other system (CECE-IF) has a 56 GHz fixed frequency LO, and the down-converted IF signal is divided into four lines with band pass filters at 4, 8, 12 and 16 GHz. The IF bandwidth of these filters has been measured to be between 0.1 and 0.2 GHz. This frequency range spans measurement positions from the core to the half radius on both sides of the magnetic axis. Post-detection, each channel is amplified by a 10 MHz bandwidth, +20 dB video amplifier and low-pass filtered by 500 KHz anti-aliasing filters. The signal from the

CECE radiometer back-end is then split into DC- and AC-coupled components and digitized with a 1 MHz sampling frequency for simultaneously measuring the mean electron temperature and electron temperature fluctuations respectively. The effective video bandwidth of each CECE channel is B_{vid}=0.5 MHz. Figure 3 shows a photo of the CECE radiometer. The signal from the plasma is split using a -3 dB, V-band directional coupler (WR-15) before being fed to each radiometer system.

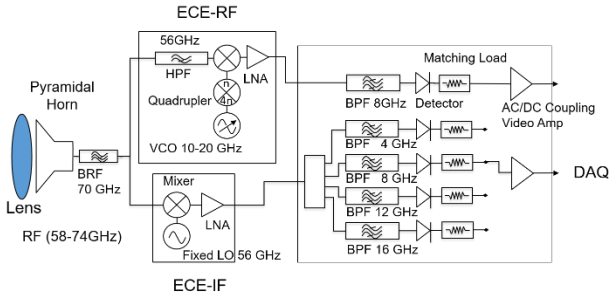

Fig. 2. Schematic view of correlation ECE radiometer in Heliotron J.

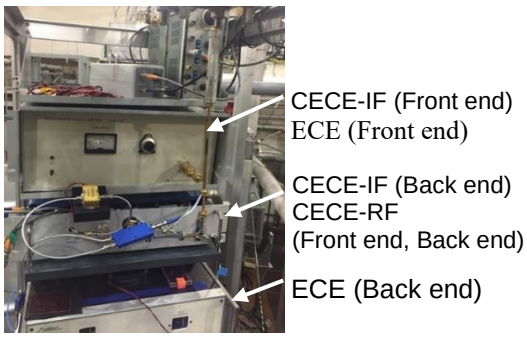

Fig. 3. Photo of CECE radiometer system in Heliotron J.

The sensitivity to electron temperature fluctuations is given by Equation (1),

$$\frac{\langle \tilde{T}_e^{\,2} \rangle}{\langle T_e \rangle^2} \geq \frac{1}{\sqrt{N}} \frac{2B_{sig}}{B_{IF}}, \qquad (1)$$

where $N=\sqrt{2B_{sig}\tau_i}$ is the number of unique samples and B_{sig} is the post-detection signal bandwidth. With a post-detection bandwidth limited by the video amplifiers, and an integration time of τ_i =0.1 sec at 1 MHz sampling frequency, the CECE radiometer is sensitive to electron temperature fluctuations above 0.4%. With a 2 cm beamwaist, the CECE diagnostic is sensitive to poloidal wavenumbers less than 1.6 cm^{-1}.

3 Laboratory tests

Pre-installation in the Heliotron J torus hall, the frequency conversion, linearity and bandwidth of the CECE radiometer were tested in the laboratory. Figure 4 shows the signal output from the CECE-RF channel with a 65 GHz Gunn oscillator applied as an input signal. The frequency of the variable local oscillator was scanned to measure the bandwidth of the CECE-RF channel, which is shown in Fig. 4. The 65 GHz input signal is downshifted by 8 GHz to 57.0 GHz, and the measured -3 dB bandwidth of the filter is 0.2 GHz.

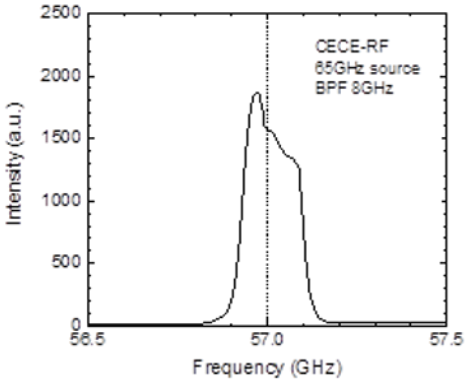

Fig. 4. Frequency conversion and bandwidth of the CECE-RF channel of the CECE radiometer. The LO was scanned to measure the CECE-RF response to a 65 GHz Gunn oscillator.

The intermediate frequency bandwidth and relative sensitivity of the CECE-IF channels was measured by applying an RF source (2-20 GHz) to the IF line of each channel. As shown in Figure 5, the measured bandwidth of each channel is between 0.1 and 0.2 GHz and the sensitivity of the radiometer decreases with higher IF frequency. Post-detection amplification is used to increase the signal measured at higher frequencies.

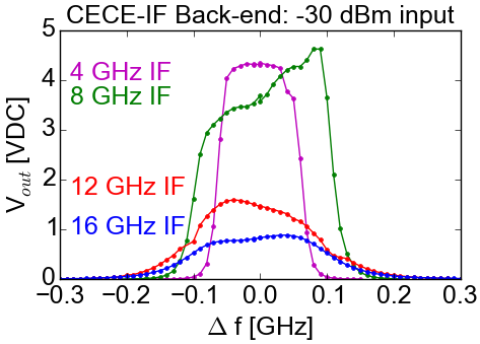

Fig. 5. Response of each CECE-IF channel to -30 dBm input.

Figure 6 show the linearity of the CECE-IF channel output voltage versus input power. The 8 GHz IF channel is used here to demonstrate the linearity of the radiometer, and it is representative of the other channels.

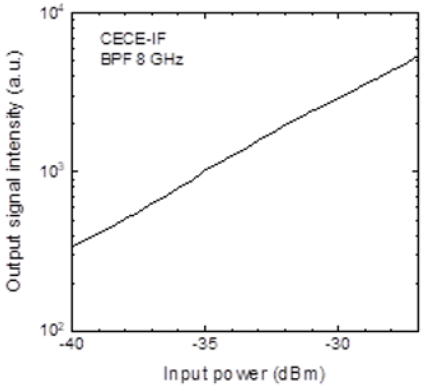

Fig. 6. Linearity of output voltage versus power applied to the 8 GHz IF line of the CECE-IF channel.

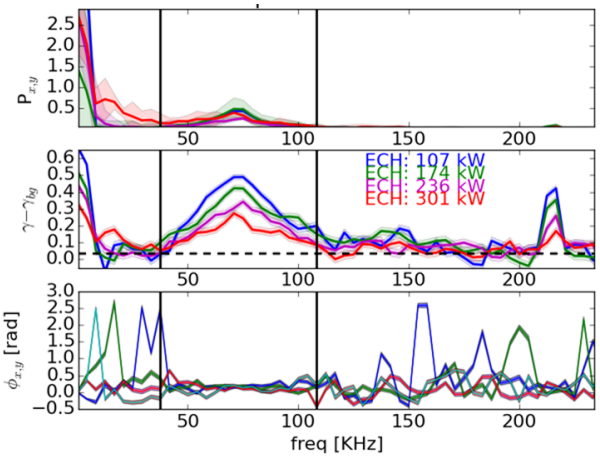

Fig. 7. Cross-power, coherence, and phase (top to bottom) between the CECE-RF and CECE-IF channels during an experiment with varying ECCD in Heliotron J.

4 Plasma experiments

The first measurements with the new radial CECE diagnostic were made in a plasma with both ECRH and NBI heating. Energetic particle modes (EPM) are excited by fast ions with NBI heating in Heliotron J, and these modes are stabilized by using counter-ECCD [20-21]. During this experiment, the CECE-RF channel was set to measure 68.3 GHz, and it was correlated over 90 ms with the 12 GHz CECE-IF channel, corresponding to a spectral separation of 0.3 GHz and a sensitivity limit of 0.41%. The cross-power, coherence, and cross-phase between the two channels are shown in Figure 7. The coherence between 40-110 KHz and 210-220 KHz measured by the CECE diagnostic decrease with increasing ECCD, consistent with the previously published results on EPM suppression in Heliotron J. The electron temperature fluctuation level is estimated by integrating the complex coherence [22], and the fluctuation level between 40-110 KHz drops from 1.8% with 107 kW of launched power to 1.1% with 301 kW of launched power. The fluctuation level of the 210-220 KHz component is below the sensitivity limit during this experiment; however, there is a low frequency component between 1-15 KHz that increases with ECCD power from 0.6% to 1.0%.

Separately, preliminary results in ECH plasmas indicate that the radial correlation length is on the order of a few mm, which is comparable to that of electron density fluctuations measured with a two-frequency reflectometer. Those results will be separately reported.

5 Summary

A new correlation ECE radiometer has been designed and installed on the Heliotron J device to measure electron temperature fluctuations. The diagnostic measures second harmonic X-mode ECE radiation between 56-72 GHz, corresponding to r/a<0.5. The system is comprised of two separate heterodyne radiometers. One radiometer has a single intermediate frequency channel and a variable local oscillator frequency, and the other has four intermediate frequency channels with a fixed local oscillator frequency. Laboratory tests indicate that the system has high spectral resolution and high-sensitivity over a large dynamic range. The first correlation ECE measurements on Heliotron J are consistent with expectations from previous experiments on Heliotron J, and the fluctuation levels measured by the CECE diagnostic are larger than the sensitivity limit of the CECE radiometer.

The authors are grateful for the Heliotron J staff for operating plasma experiments. This work was carried out with the support from the auspices of the Collaboration Program of the Laboratory for Complex Energy Processes, IAE, Kyoto Univ., the NIFS Collaborative Res. Program (NFIS10KUHL030), the NIFS/NINS project of Formation of International Network for Scientific Collaboration, JSPS Postdoctoral Fellowships for Research in Japan and JSPS Grant-in-Aid for Scientific Research (B) 18H01199. This work has been carried out within the framework of the EUROfusion Consortium and has received funding form the Euratom research and training programme 2014-2018 under grant agreement No 633053. The views and opinions expressed herein do not necessarily reflect those of the European Commission.

References

1. F. Ryter, *et al.*, Phys. Rev. Lett. **95**, 085001 (2005)
2. J. C. DeBoo, *et al.*, Phys. Plasmas **19**, 082518 (2012)
3. G. M. Weir, *et al.*, Phys. Plasmas **22**, 056107 (2015)
4. C. Watts, Fusion Sci. Technol. **52**, 176 (2007)
5. S. Sattler and H. J Hartfuss, "Evidence for Temperature Fluctuations in the W7-AS Stellarator", presented at Int. School of Plasma Physics, Varenna, Italy, 1993
6. R. F. Gandy, *et al.*, "Measurement of Electron Cyclotron Emission Fluctuations in TEXT", presented at Int. School of Plasma Physics, Varenna, Italy, 1993
7. C. Watts, *et al.*, Rev. Sci. Instrum. **66**, 451 (1995)
8. M. Kwon, *et al.*, Rev. Sci. Instrum. **63**, 4633 (1992)
9. G. Cima, *et al.*, Phys. Plasmas **2**, 720 (1995)
10. S. Sattler, H. J. Hartfuss adn W7-AS team, Phys. Rev. Lett. **72**, 653 (1994)
11. A. E. White, *et al.*, Phys. Plasmas **15**, 056116 (2008)
12. A. E. White, *et al.*, Phys. Plasmas **17**, 020701 (2010)
13. S. Freethy, *et al.*, Rev. Sci. Instrum. **87**, 11E102 (2016)
14. S. Freethy, *et al.*, Phys. Plasmas **25**, 055903 (2018)
15. G. M. Weir, *et al.*, this workshop
16. M. Wakatani, *et al.*, Nucl. Fusion **40**, 569 (2000)
17. T. Obiki, *et al.*, Nucl. Fusion **41**, 833 (2001)
18. K. Nagasaki, *et al.*, Contrib. Plasma Phys. **50**, 656 (2010)
19. K. Nagasaki, *et al.*, Fusion Eng. Design **34**, 463 (1997)
20. K. Nagasaki, *et al.*, Nucl. Fusion **53**, 113041 (2013)
21. S. Yamamoto, *et al.*, Nucl. Fusion **57**, 126065 (2017)
22. A. J. Creely, *et. al.*, Rev. Sci. Instrum. **89**, 053503 (2018)